R. & M. No. 3716

R. & M. No. 3716

MINISTRY OF DEFENCE (PROCUREMENT EXECUTIVE)

AERONAUTICAL RESEARCH COUNCIL
REPORTS AND MEMORANDA

The Load near the Apex of a Lifting Swept Wing in Linearised Subsonic Flow

By PATRICIA J. DAVIES

Aerodynamics Dept., RAE Farnborough

LONDON: HER MAJESTY'S STATIONERY OFFICE

1973

PRICE £1·20 NET

The Load near the Apex of a Lifting Swept Wing in Linearised Subsonic Flow

By PATRICIA J. DAVIES

Aerodynamics Dept., RAE Farnborough

Reports and Memoranda No. 3716*
January, 1972

Summary

Recent work of Hewitt on subsonic lifting-surface theory for wings with pointed apices has shown that representing both the singularity in the load at the apex and the detailed behaviour of the load near the apex leads to large increases in the accuracy of collocation methods.

The strength of the singularity has been found in earlier calculations as a function of the apex angle of the wing. These calculations are extended here to include the nonsingular factor in the load, which also depends on the apex angle. Interpolation formulae are obtained, which provide an accurate closed-form approximation to the behaviour of the load distribution near the apex for all apex angles.

LIST OF CONTENTS

* Replaces RAE Technical Report 72031-A.R.C.33 584.

1. Introduction

In the calculation of the subsonic flow past lifting wings, several collocation methods[1] give satisfactory solutions of the classical lifting-surface theory problem for wings with 'regular' planforms, i.e. planforms whose leading and trailing edges have no discontinuities in slope. However, when applied to planforms whose leading edges are cranked, these methods are less satisfactory, as the singular behaviour of the load predicted by linearised theory near the crank is not represented.

In the case of a swept wing with a pointed apex, i.e. a wing whose leading edge has a crank at the centre-section, the strength of the singularity in the load as the apex is approached along a ray is now known[2,3,4] and has been incorporated into a lifting-surface calculation for a particular planform by Hewitt[5]. However, Hewitt has also shown that substantially better accuracy is obtained using an appropriate representation of the angular variation of the load near the apex, as well as its variation along the rays.

Accordingly, the earlier calculations[2,3] concerning the singularity in the load have been extended to provide a representation of the behaviour of the load near the apex as a function of both the polar distance and the polar angle about the apex, for all swept back wings.

Germain[6] has shown that, according to the linearised theory of subsonic flow, the velocity potential in the neighbourhood of the apex of a lifting swept wing is dominated by a term which is an eigensolution of the differential equation and boundary conditions which govern the velocity potential of subsonic flow past an infinite plane sector with the same semi-apex angle as the wing[2]. The velocity potential of the flow past the infinite plane sector has eigensolutions of the form

$$\phi_m = r^{\nu_m} f_m(\vartheta, \omega) \qquad m = 0, 1, 2 \ldots$$

where r is the distance from the apex, ϑ and ω are angular coordinates and f_m and ν_m depend on the semi-apex angle γ. The dominant eigensolution is the one for which the value of the exponent ν lies between zero and one. We shall write this without suffices as

$$\phi = r^{\nu} f(\vartheta, \omega).$$

As the load is proportional to the streamwise derivative of the velocity potential, this first eigensolution governs the singular behaviour of the load ΔC_p. The dominant term in the load can be written as

$$\Delta C_p = r^{\nu - 1} u^{-\frac{1}{2}} F(u),$$

where u is a coordinate on the wing measured from the leading edges, so that the factor $u^{-\frac{1}{2}}$ is the familiar square root singularity in the load at the leading edge. The factor $F(u)$ is a regular function of u depending on the semi-apex angle γ. It is this function that is required, as well as ν, in order to describe the detailed behaviour of the load near the apex.

Calculations of the exponent ν for a large range of semi-apex angles γ have previously been reported[2]. The method used involved the solution of a finite difference approximation to a second order partial differential equation for f in which ν was an eigenvalue. The present report presents calculations of an approximate expression for $F(u)$ from this finite difference solution for f, in the form of a cubic polynomial in u

$$F(u) = a_0 + a_1 u + a_2 u^2 + a_3 u^3,$$

where the coefficients a_i are functions of the semi-apex angle γ. This method, described in Section 3 and Appendix I, enables $F(u)$ to be found for any semi-apex angle which is not too small. For smaller semi-apex angles, an expression for $F(u)$ can be found from the series expansion for ϕ for very slender wings given by Brown and Stewartson[3], and this is described in Section 4.1. This expression for $F(u)$ can also be approximated by a cubic polynomial in u. The function $F(u)$ can be found analytically for the cases when $\gamma = 0$ or $\pi/2$, and these cases are considered in Sections 4.2 and 4.3.

Cubic polynomial approximations for $F(u)$ have been found using the above methods for a range of values of semi-apex angle between 0 and $\pi/2$, and the coefficients a_i of these polynomials are given in Table 1. In order that the behaviour of the load near the apex can be found easily and quickly for any semi-apex angle γ between 0 and $\pi/2$, the variation with γ of ν and each of the coefficients a_i has been represented by a seventh order polynomial in γ. These are given in Section 5.

To assess the overall accuracy of the method, $F(u)$ has been calculated using two other methods[8,9] for the case $\gamma = \pi/4$. A comparison of these results with those of the present method, *see* Table 2, shows very good agreement.

Since Ref. 2 was published, additional values of the exponents ν_m have been calculated by different methods and the opportunity is taken in Appendix III and Figs. 9 to 12 of this report to compare the first two exponents for $0 \leqslant \gamma \leqslant \pi$, as calculated by the methods of Brown and Stewartson[3], Taylor[4] and Sack[12].

2. The Equation for the Load

According to the linearised theory, the velocity potential of the subsonic flow past the apex of a lifting swept wing is dominated by a term which is an eigensolution of the corresponding problem for an infinite plane sector[6]. The eigensolution takes the form

$$\phi = r^{\nu} f(\vartheta, \omega), \tag{1}$$

where r is the difference from the apex, f is a function of the polar angles ϑ and ω, and ν is a constant depending only on the semi-apex angle γ, lying in the range $0 \leqslant \nu \leqslant 1$. As an eigensolution, ϕ is only determined within a multiplicative constant. This means that the form of the load near the apex of the wing is given by the eigensolution, though its magnitude, which depends on conditions over the whole wing, must be found from a lifting-surface theory calculation. Previously, a table of values of ν for different values of γ was calculated[2]. This calculation has now been extended to find the eigenfunction f on the sector and hence the form of the wing load ΔC_p.

The rectangular coordinate system (y_1, y_2, y_3) of Ref. 1 is used, with $y_3 = 0$ the plane of the sector, $y_2 = 0$ the plane of symmetry of the flow, and the apex of the sector at the origin 0, see Fig. 1.

The load ΔC_p at a point (y_1, y_2) is given, according to linearised theory, by

$$\Delta C_p(y_1, y_2) = 4 \frac{\partial \phi}{\partial y_1}(y_1, y_2)\bigg|_s \tag{2}$$

where the suffix s denotes evaluation on the upper surface of the sector. Thus when $\phi = r^{\nu} f$

$$\Delta C_p(y_1, y_2) = 4 \left\{ r^{\nu} \frac{\partial f}{\partial y_1} + \nu r^{\nu - 1} f \frac{y_1}{r} \right\}_s . \tag{3}$$

In terms of u, a coordinate on the sector, as used by Hewitt[5], where

$$u = \frac{\cos\theta - \cos\gamma}{1 - \cos\theta \cos\gamma}$$

and (4)

$$\cos\theta = \frac{y_1}{r},$$

equation (3) for ΔC_p can be written

$$\Delta C_p = \frac{r^{\nu - 1}}{u^{\frac{1}{2}}} \tilde{F}(u) \tag{5}$$

where

$$\tilde{F}(u) = \left\{4u^{\frac{1}{2}} r \frac{\partial f}{\partial y_1} + 4\nu u^{\frac{1}{2}} \frac{y^1}{r} f\right\}_s . \tag{6}$$

The factor $u^{-\frac{1}{2}}$ represents the usual singularity of ΔC_p at the leading edges, so that $\tilde{F}(u)$ is a regular function of u. f, and hence $\tilde{F}$, are determined only to a multiplicative constant, and it is convenient to remove this arbitrary factor from the functions we consider by dividing them by their values at the centreline of the sector, where $u = 1$. $r\partial f_s/\partial y_1$ is zero when $u = 1$ (and $y_1 = 0$, $\theta = 0$) since on the centreline, f_s is independent of y_1, and therefore $\tilde{F}$, at $u = 1$, has the value

$$\tilde{F}(1) = 4\nu f_s(1).$$

We therefore consider the behaviour of the load near the apex given by the equation

$$\Delta C_p(r, u) = \frac{r^{\nu - 1}}{u^{\frac{1}{2}}} F(u) \tag{7}$$

where

$$F(u) = \left\{\frac{u^{\frac{1}{2}} r}{\nu} \frac{\partial f}{\partial y_1} + u^{\frac{1}{2}} \frac{y_1}{r} f\right\}_s \tag{8}$$

and $f_s(u)$ is normalised by its value at $u = 1$. Thus the behaviour of the load can be deduced from the behaviour of f on the sector.

3. Calculation of the Velocity Potential Eigenfunction and the Load

The behaviour of f on the sector can be determined by the method used in the earlier calculation[2] for ν. Full details of this calculation are given in Ref. 2, and the method is summarised below.

The velocity potential ϕ satisfies Laplace's equation

$$\frac{\partial^2 \phi}{\partial y_1^2} + \frac{\partial^2 \phi}{\partial y_2^2} + \frac{\partial^2 \phi}{\partial y_3^2} = 0, \tag{9}$$

with the boundary conditions that ϕ is symmetrical about $y_2 = 0$ and that in the plane of the sector, $y_3 = 0$,

$$\frac{\partial \phi}{\partial y_3} = 0 \qquad \text{for} \frac{|y_2|}{\tan \gamma} < y_1$$

and

$$\phi = 0 \qquad \text{for} \frac{|y_2|}{\tan \gamma} > y_1 . \tag{10}$$

In a system of orthogonal curvilinear coordinates (r, θ_0, τ) such as that used by Legendre[7],

$$y_1 = \frac{r \cos \theta_0}{\cosh \tau}, \qquad y_2 = \frac{r \sin \theta_0}{\cosh \tau}, \qquad y_3 = r \tanh \tau \quad \text{and} \quad r = (y_1^2 + y_2^2 + y_3^2)^{\frac{1}{2}},$$

the substitution of the form (1) of the velocity potential

$$\phi = r^{\nu} f(\tau, \theta_0)$$

into equation (9) leads to the equation

$$\frac{\partial^2 f}{\partial \tau^2} + \frac{\partial^2 f}{\partial \theta_0^2} + \frac{\nu(\nu + 1)}{\cosh^2 \tau} f = 0.$$

This is a second order partial differential equation for f in the two variables τ and θ_0, in which ν is a parameter.

A non-conformal transformation of coordinates from (θ_0, τ) to (R, φ) is then made so that the domain of the problem becomes rectangular, as shown in Fig. 2. The sector corresponds to the line $R = 1$ and the line $R = 0$ to infinity upstream. The equations describing the transformation are given in full in Ref. 2. However, on the sector, φ is related to the coordinates θ and u by

$$\cos \varphi = \frac{\tan \theta/2}{\tan \gamma/2} = \left(\frac{1 - u}{1 + u}\right)^{\frac{1}{2}}. \tag{11}$$

In the (R, φ) coordinate system, the equation to be solved becomes

$$\psi(R, \varphi)\left\{\frac{\partial^2 f}{\partial R^2} + \frac{1}{R}\frac{\partial f}{\partial R} + \frac{1}{R^2}\frac{\partial^2 f}{\partial \varphi^2}\right\} + \nu(\nu + 1) f = 0 \tag{12}$$

where

$$\psi(R, \varphi) = \frac{(R^2 + 0{\cdot}25(R^4 + 2R^2 \cos 2\varphi + 1)\tan^2 \gamma/2)^2}{(R^4 + 1 - 2R^2 \cos 2\varphi)\tan^2 \gamma/2}.$$

The boundary conditions on f are derived from those for ϕ in equation (10). They apply at the boundary of the domain and are

$$\begin{aligned}
&\text{(i)} && f = 0 \text{ on } \varphi = 0, 0 \leqslant R \leqslant 1 \text{ and on } R = 0, 0 \leqslant \varphi \leqslant \pi/2, \\
&\text{(ii)} && \partial f/\partial R = 0 \text{ on } R = 1, 0 \leqslant \varphi \leqslant \pi/2, \\
&\text{(iii)} && \partial f/\partial \varphi = 0 \text{ on } \varphi = \pi/2, 0 \leqslant R \leqslant 1.
\end{aligned} \tag{13}$$

Since equation (12) and the boundary conditions (13) are homogeneous, non-zero solutions only exist for special values of ν, the eigenvalues of the problem.

We find approximations to these eigenvalues and the associated eigensolutions by using a finite difference approximation to equation (12) at points of a grid over the domain. This leads to a matrix equation

$$(E_0 - \lambda I)\mathbf{f} = 0$$

where

$$\lambda = \nu(\nu + 1),$$

E_0 is a matrix with known coefficients, and $\mathbf{f}$ a vector whose elements are the values of a finite difference approximation to f at the gridpoints. Thus for a non-trivial solution for $\mathbf{f}$, λ must be an eigenvalue of the

matrix E_0 and $\mathbf{f}$ the corresponding eigenvector. A computer program has been written[2] to find λ and $\mathbf{f}$ for a given semi-apex angle γ and grid size, using inverse iteration[10]. Details of the program are given in Appendix I. Those elements of $\mathbf{f}$ corresponding to grid points on the line $R = 1$ are the values of the finite difference approximation to f at the gridpoint values of φ on the wing surface.

The variation of f with u is illustrated in Fig. 3 for three semi-apex angles. f is zero at the leading edge where $\varphi = 0$, $u = 0$ and $\theta = \gamma$, from the boundary conditions (13), and has been normalised so that its value is unity at the sector centreline, where $\varphi = \pi/2$, $u = 1$ and $\theta = 0$.

F can be expressed as a function of φ with the help of the following relationships between the coordinate systems in the plane of the sector:

$$\frac{y_1}{r} = \frac{1 - \tan^2(\gamma/2)\cos^2\varphi}{1 + \tan^2(\gamma/2)\cos^2\varphi},$$

$$u = \frac{\sin^2\varphi}{1 + \cos^2\varphi}$$

and

$$\left.\frac{\partial\varphi}{\partial y_1}\right|_{y_2 \text{ constant}} = \frac{1}{r}\cot\varphi.$$

Then, from equation (8),

$$F(\varphi) = \left\{\frac{u^{\frac{1}{2}}r}{\nu}\frac{\partial f}{\partial\varphi}\left.\frac{\partial\varphi}{\partial y_1}\right|_{y_2 \text{ constant}} + u^{\frac{1}{2}}\frac{y_1}{r}f\right\}_s$$

and thus

$$F(\varphi) = \frac{1}{\nu}\frac{\cos\varphi}{(1 + \cos^2\varphi)^{\frac{1}{2}}}\frac{\partial f_s}{\partial\varphi} + \frac{\sin\varphi}{(1 + \cos^2\varphi)^{\frac{1}{2}}}\left\{\frac{1 - \tan^2(\gamma/2)\cos^2\varphi}{1 + \tan^2(\gamma/2)\cos^2\varphi}\right\}f_s. \tag{14}$$

The original computer program has been extended to calculate the values of $F(\varphi)$ at the gridpoint values of φ, from equation (14), using a previously calculated, accurate value for the eigenvalue ν and Lagrangian differentiation to calculate $\partial f_s/\partial\varphi$ at the gridpoints. It was found that a seven-point differentiation formula was sufficiently accurate, as it gave the same value for $F(\varphi)$, to five significant figures, as a nine-point formula, over the range of values of φ.

A cubic polynomial in u was then fitted through the values of F using a least-squares curve-fitting method, keeping the values of F at $u = 0$ and $u = 1$ fixed. This fitted polynomial predicts the variation of F with u very closely, as the residuals, i.e. the differences between the fitted and actual values of F, are mostly less than 0·00002, and the largest residual is only 0·00006. Thus for a specified semi-apex angle γ and mesh size, an approximation $\bar{F}$ for F is obtained:

$$\bar{F}(u) = \bar{a}_0 + \bar{a}_1 u + \bar{a}_2 u^2 + \bar{a}_3 u^3 \tag{15}$$

where

$$\sum_{i=0}^{3}\bar{a}_i = 1 \tag{16}$$

and

$$\bar{a}_0 = \frac{1}{\nu}\frac{1}{\sqrt{2}}\left.\frac{\partial f}{\partial\varphi}\right|_{\varphi=0}.$$

A numerical approximation for F appropriate to an infinitely small mesh size is then obtained by extrapolation from a series of polynomials $\bar{F}(u)$ calculated for different mesh sizes. A square mesh with l equally spaced gridpoints along each side was used, l being 18, 19 or 20. It was found that the variation of each coefficient $\bar{a}_i$ with l could be approximated by

$$\bar{a}_i(\gamma, l) = \frac{c_i}{l^{k_i}} + a_i(\gamma), \tag{17}$$

where c_i and k_i are constants for a particular γ and $a_i(\gamma)$ is the limit of the $\bar{a}_i(\gamma, l)$ as l tends to infinity. The difference between this limiting value of a_i and the $\bar{a}_i$ for the largest mesh size was generally of the order of 0·001, but with a_2 and a_3 it increased to 0·008 for γ near 90 degrees. Values of a_0, a_1 and a_2 were calculated using the formula (17), and then a_3 was found to satisfy the condition (16)

$$\sum_{i=0}^{3} a_i = 1, \tag{18}$$

though, in practice, this value of a_3 differed by less than 0·0001 from that obtained from the formula (17). The polynomial

$$a_0 + a_1 u + a_2 u^2 + a_3 u^3 \tag{19}$$

is then a numerical approximation of the function F, at the specified semi-apex angle.

Such polynominals for F have been calculated for a number of values of γ between 27 and 90 degrees, and the coefficients a_i of these are given in Table 1. However, the present method is unsuitable for low values of γ, since the extrapolation to zero mesh size becomes unreliable. For these values of γ, a polynomial representation for F has been obtained in Section 4.1, using a series expansion[3] for ϕ for small γ.

The accuracy of the present method has been investigated by comparisons with other methods at $\gamma = 27$, 45 and 90 degrees. At $\gamma = 27$ degrees, it is shown that the present method and the method for small γ gives values of F differing by not more than 0·00008. In Appendix II, F calculated by the present method for $\gamma = 45$ degrees is compared with F calculated by Taylor[9] and by Brown[8], who has calculated f_s at this one semi-apex angle. This shows very good agreement between the functions calculated by different methods, the largest difference being 0·00015. Similarly good agreement is obtained for $\gamma = 90$ degrees, the present method giving the result

$$F(u) = 1{\cdot}00000 - 0{\cdot}00005u + 0{\cdot}00017u^2 - 0{\cdot}00012u^3,$$

whereas the analytical result is shown in Section 4.3 to be

$$F(u) = 1.$$

The functions $F(u)$ for three semi-apex angles are illustrated in Fig. 4.

4. The Load for some Special Cases

The numerical method given in the previous section provides a cubic polynomial approximation for F over a large range of values of semi-apex angles γ between 27 and 90 degrees. To provide a representation of F over the range of γ from zero to $\pi/2$, the behaviour of F for small values of γ was deduced from a series expansion for f due to Brown and Stewartson[3], and expressions for F when $\gamma = 0$ and $\pi/2$ have been found analytically.

4.1. The Load for Small Apex Angles

When γ is small, the behaviour of $F(u)$ can be derived from the series expansion for ϕ calculated by Brown and Stewartson[3]. They express ϕ as

$$\phi = r^{\nu} G(\sigma) H(\zeta)$$

where, on the sector,

$$\zeta = \sec\gamma \frac{y_1}{r} = \sec\gamma \cos\theta,$$

$\sigma = 1$, G is constant, and so

$$f_s = H(\zeta)/H(\zeta = k).$$

Letting

$$k = \sec\gamma = 1 + p$$

$$\zeta = 1 + p\mu, \tag{20}$$

Brown and Stewartson derived a series expansion[8] for H in powers of p:

$$H(\mu) = \mu^{\frac{1}{2}} + \tfrac{1}{4}p\mu^{\frac{3}{2}} - p^2\{\tfrac{3}{8}\mu^{\frac{3}{2}} + \tfrac{1}{32}\mu^{\frac{5}{2}}\} + O\{p^3(\log p)^2\}.$$

Thus, neglecting terms of order higher than p^2

$$f_s = \frac{\mu^{\frac{1}{2}} + \tfrac{1}{4}p\mu^{\frac{3}{2}} - p^2\{\tfrac{3}{8}\mu^{\frac{3}{2}} + \tfrac{1}{32}\mu^{\frac{5}{2}}\}}{(1 + \tfrac{1}{4}p - \tfrac{13}{32}p^2)} \tag{21}$$

where f_s is normalised with respect to its value at $\mu = 1, \theta = 0, u = 1$.

On the sector, the coordinates are related by

$$\frac{y_1}{r} = \frac{1 + ku}{k + u}$$

and

$$\mu = \frac{u(1 + k)}{k + u}, \tag{22}$$

so that

$$\frac{d\mu}{du} = \frac{k(1 + k)}{(k + u)^2}$$

and

$$r\frac{\partial u}{\partial y_1} = 1 - u^2.$$

From equation (8),

$$F(u) = \left\{ \frac{u^{\frac{1}{2}}}{v} \frac{\partial f}{\partial \mu} \frac{d\mu}{du} r \frac{\partial u}{\partial y_1} + u^{\frac{1}{2}} \frac{y_1}{r} f \right\}_s .$$

Substituting into this equation from equations (20), (21) and (22) we obtain an expression for F for small γ:

$$\begin{aligned} F(u) = {} & \frac{(1+k)^{\frac{1}{2}}}{(1+\frac{1}{4}p - \frac{13}{32}p^2)(k+u)^{\frac{3}{2}}} \\ & \times \left[\frac{(1-u^2)k}{2v} \left(1 + \frac{3}{4} \frac{pu(1+k)}{(k+u)} - p^2 \left[\frac{9}{8} \frac{u(1+k)}{(k+u)} + \frac{5}{32} \left\{ \frac{u(1+k)}{k+u} \right\}^2 \right] \right) \right. \\ & \left. + u(1+ku) \left(1 + \frac{1}{4} \frac{pu(1+k)}{k+u} - p^2 \left[\frac{3}{8} \frac{u(1+k)}{(k+u)} + \frac{1}{32} \left\{ \frac{u(1+k)}{k+u} \right\}^2 \right] \right) \right] \end{aligned} \tag{23}$$

in which terms of order higher than p^2 have been neglected.

This expression (23) is rather cumbersome for practical use, and so, in line with the method of the previous section, F has been approximated numerically for certain values of γ by a cubic polynomial of the form

$$F(u) = a_0 + a_1 u + a_2 u^2 + a_3 u^3 .$$

Values of the coefficients a_i are given in Table 1 for values of γ up to 27 degrees. At 27 degrees, the agreement between the method of Section 3 and this method of Section 4.1 is extremely good, the former method giving

$$F(u) = 0{\cdot}71740 + 0{\cdot}33665u - 0{\cdot}06948u^2 + 0{\cdot}01543u^3$$

and the method for small γ giving

$$F(u) = 0{\cdot}71732 + 0{\cdot}33708u - 0{\cdot}07005u^2 + 0{\cdot}01565u^3 .$$

This gives confidence that an expression for F can be found to sufficient accuracy over the whole range of semi-apex angles using one of these two methods.

4.2. The Load for a Vanishing Apex Angle

The function $F(u)$ corresponding to a vanishingly small semi-apex angle can be calculated analytically from the series expansion[3] for ϕ for small angles of γ. At $\gamma = 0$, v has the value 1, $k = 1$, and $p = 0$. Substituting these values into the expression (23) for $F(u)$, we obtain

$$F(u) = \left(\frac{1+u}{2} \right)^{\frac{1}{2}} . \tag{24}$$

Approximating this function in keeping with the representation of $F(u)$ by a cubic polynomial over the whole range of semi-apex angles, we obtain the expression

$$F(u) = 0{\cdot}70711 + 0{\cdot}35162u - 0{\cdot}07589u^2 + 0{\cdot}01716u^3 .$$

The functions $f_s(u)$ and $F(u)$ when $\gamma = 0$ are illustrated in Figs. 3 and 4.

4.3. The Load for an Unswept Wing

When $\gamma = \pi/2$, the sector becomes a half-plane and the flow is therefore two-dimensional and well-known[11]. The velocity potential tends to zero like the square root of the distance from the leading edge and the load tends to infinity like the reciprocal of the square root of the distance from the leading edge. Thus

$$\phi \propto y_1^{\frac{1}{2}}$$

$$= r^{\frac{1}{2}} \cos^{\frac{1}{2}} \theta.$$

When $\gamma = \pi/2$, $\cos\theta = u$ from equation (4).

So

$$\phi \propto r^{\frac{1}{2}} u^{\frac{1}{2}},$$

ν has the value $\frac{1}{2}$ and $f_s = \cos^{\frac{1}{2}} \theta = u^{\frac{1}{2}}$.

Also the load

$$\Delta C_p \propto \frac{1}{y_1^{\frac{1}{2}}} \propto \frac{r^{-\frac{1}{2}}}{\cos^{\frac{1}{2}} \theta} = \frac{r^{\nu-1}}{u^{\frac{1}{2}}}.$$

Therefore, when $\gamma = \pi/2$, $F(u)$ is identically equal to one.

The functions $f_s(u)$ and $F(u)$ for $\gamma = \pi/2$ are illustrated in Figs. 3 and 4.

5. Interpolation Formulae to give the Load for a General Semi-Apex Angle

The methods of Sections 3 and 4 enable an expression for $F(u)$ to be calculated for any specified semi-apex angle γ in the range $0 \leqslant \gamma \leqslant \pi/2$. However, these methods are too complicated and time-consuming to be incorporated into a lifting-surface program, and a much simpler and quicker method of calculating ν and $F(u)$ for a general value of semi-apex angle γ is required for this purpose.

A suitable method is interpolation from quantities ν and $F(u)$ known at tabular values of γ. The interpolation for $F(u)$ can be based on the expression by which $F(u)$ is approximated by the methods of Sections 3 and 4,

$$F(u, \gamma) = a_0(\gamma) + a_1(\gamma)u + a_2(\gamma)u^2 + a_3(\gamma)u^3. \tag{25}$$

This approximation (25) has been used for all values of γ, so that interpolation is possible over the complete range of values of γ, although an approximation of the form

$$F(u) = (1 + u)^{\frac{1}{2}} \times (\text{a polynomial in } u)$$

would be more appropriate for very small γ, i.e. γ less than $\pi/12$.

Cubic polynomials for $F(u)$ of the form (25) have been found at equally spaced values of γ and are given in Table 1, together with the value of ν used in the calculation of F. The variation of ν and each of the coefficients a_0, a_1 and a_2 with γ has been approximated by a seventh order polynomial using a least-squares curve-fitting method. The variation of a_3 with γ can then be found, since from equation (18)

$$\sum_{i=0}^{3} a_i(\gamma) = 1.$$

The polynomials for v and the coefficients a_i are,

$$\left.\begin{aligned}
v &= 0{\cdot}5 + (1-\rho)(0{\cdot}5 + 0{\cdot}487495\rho + 0{\cdot}058458\rho^2 - 0{\cdot}679288\rho^3 - 2{\cdot}782556\rho^4 \\
&\quad + 5{\cdot}413016\rho^5 - 2{\cdot}513314\rho^6), \\
a_0 &= 1 + (1-\rho)(-0{\cdot}29289 - 0{\cdot}289532\rho - 0{\cdot}306319\rho^2 - 0{\cdot}595218\rho^3 + 3{\cdot}447159\rho^4 \\
&\quad - 3{\cdot}751175\rho^5 + 1{\cdot}287896\rho^6), \\
a_1 &= (1-\rho)(0{\cdot}35162 + 0{\cdot}355542\rho + 0{\cdot}238705\rho^2 + 1{\cdot}392805\rho^3 - 6{\cdot}210993\rho^4 \\
&\quad + 6{\cdot}285457\rho^5 - 2{\cdot}000932\rho^6), \\
a_2 &= (1-\rho)(-0{\cdot}07587 - 0{\cdot}080020\rho - 0{\cdot}005846\rho^2 - 0{\cdot}568412\rho^3 + 2{\cdot}708097\rho^4 \\
&\quad - 2{\cdot}425370\rho^5 + 0{\cdot}564653\rho^6)
\end{aligned}\right\} \quad (26)$$

and

$$\left.\begin{aligned}
a_3 &= (1-\rho)(0{\cdot}01714 + 0{\cdot}014010\rho + 0{\cdot}073460\rho^2 - 0{\cdot}229175\rho^3 + 0{\cdot}055737\rho^4 \\
&\quad - 0{\cdot}108912\rho^5 + 0{\cdot}148383\rho^6)
\end{aligned}\right\}$$

where $\rho = \left(\frac{\gamma}{\pi/2}\right)$.

The values of the coefficients a_i calculated from these polynomials (26) at the tabular values of γ are close to the accurately calculated values of the a_i given in Table 1, the difference mostly being less than 0·0001 and the largest difference 0·00022. The dependence of the coefficients a_i on γ is therefore well represented by the polynomials (26), and is illustrated in Figs. 5 to 8.

6. Conclusions

The method[2] used previously to calculate the singular behaviour of the load as the apex is approached along a ray has been extended to calculate how the load near the apex varies with the polar angle. The results have been expressed in the form of a double polynomial in the semi-apex angle and an angular coordinate on the wing, so that they may readily be incorporated in lifting surface programs. The accuracy has been assessed by comparison with the known analytic solution for the upswept wing, with a series expansion for slender wings and with two independent calculations available for 45 degree swept wings.

Comparison with other calculations has confirmed the accuracy of the previous evaluation of the exponent of the singularity at the apex of a swept back wing.

LIST OF SYMBOLS

a_0, a_1, a_2, a_3	Coefficients of polynomial for $F(u)$, *see* equation (17)
$\bar{a}_0, \bar{a}_1, \bar{a}_2, \bar{a}_3$	Coefficients of polynomial for $\bar{F}(u)$, *see* equation (15)
ΔC_p	Wing load
E_0	Matrix in finite difference solution
f	Factor in the velocity potential ϕ
f_m	Factor in the velocity potential eigensolution ϕ_m
f_i	Value of f at ith grid point
$\mathbf{f}$	Column vector $\{f_1, \ldots, f_i, \ldots f_{II}\}$
$F(u)$	Factor in load
$\bar{F}(u)$	Finite difference approximation for $F(u)$
G, H	Factors in the velocity potential ϕ in Section 4.1
k	$= \sec \gamma$
l	Number of gridpoints along side of mesh
p	$= k - 1$, *see* equation (20)
r	Distance from apex of sector
R, φ	Coordinate system for finite difference solution, *see* Section 3 and Fig. 2
u	Coordinate on sector, *see* equation (4)
y_1, y_2, y_3	Cartesian coordinate system, *see* Fig. 1
γ	Semi-apex angle
θ	$= \cos^{-1}(y_1/r)$
θ_0, τ	Orthogonal curvilinear coordinates, *see* Section 3
λ	Eigenvalue of finite difference solution
μ	$= (\zeta - 1)/p$, *see* equation (20)
ν	Exponent of distance factor in the velocity potential ϕ, $(= \nu_0)$
ν_m	Exponents of distance factor in the velocity potential eigensolution ϕ_m

ρ	$= 2\gamma/\pi$
σ, ζ	Coordinate system, *see* Section 4.1
ϕ	First eigensolution of the disturbance velocity potential of flow past a sector
ϕ_m	Eigensolutions of the disturbance velocity potential of flow past a sector
φ	*See* R, φ

Suffix

s	Denotes evaluation on the upper surface of the sector

REFERENCES

No.	*Author(s)*	*Title, etc.*
1	H. C. Garner, B. L. Hewitt and T. E. Labrujere	Comparison of three methods for the evaluation of subsonic lifting-surface theory. A.R.C. R. & M. 3597 (1968).
2	Patricia J. Rossiter	The linearised subsonic flow over the centre-section of a lifting swept wing. A.R.C. R. & M. 3630 (1969).
3	S. N. Brown and K. Stewartson	Flow near the apex of a plane delta wing. *Jl.I.M.A.*, 5, 206–216 (1969).
4	R. S. Taylor	A new approach to the delta wing problem. *Jl. I.M.A.*, *7*, 337–347 (1971).
5	B. L. Hewitt and W. Kellaway	Developments in the lifting surface theory : treatment of symmetric planforms with a leading edge crank in subsonic flow. BAC Ltd., Preston Division, Report Ae 313 (1971).
6	P. Germain	Sur l'écoulement subsonique au voisinage de la pointe avante d'une aile delta. *La Recherche Aéronautique 44*, 3–8 (1955).
7	R. Legendre	Écoulement subsonique transversal à un secteur angulaire plan. *C.R. Acad. Sci.*, 1716–18, 26 November 1956.
8	S. N. Brown	Private communication.
9	R. S. Taylor	Private communication.
10	L. Fox	*An introduction to numerical linear algebra.* Oxford, Clarendon Press, pp. 224–225 (1964).
11	B. Thwaites	*Incompressible aerodynamics.* Oxford University Press, pp. 116, 299 (1960).
12	R. Sack	Variational solutions for eigenvalues of single and coupled Lamé equations. *Jl. I.M.A.*, 10, 279–288 (1972).

APPENDIX I

Calculation of the Eigenfunction of the Matrix

The eigenvalue λ of the matrix E_0 of smallest modulus and its corresponding eigenfunction $\mathbf{f}$ are calculated using an inverse iteration scheme[10]. This scheme finds the eigenvalue with smallest modulus of a matrix A by successively solving the matrix equation

$$A\mathbf{y}^{(p)} = \mathbf{y}^{(p-1)},$$

for the vector $\mathbf{y}^{(p)}$, where $\mathbf{y}^{(0)}$ is arbitrary. If the matrix A is of order n, and has eigenvectors $\mathbf{x}^{(r)}$ and eigenvalues α_r, where $r = 1, 2 \ldots n$, then an arbitrary vector $\mathbf{y}^{(0)}$ can be expressed in the form

$$\mathbf{y}^{(0)} = \sum_{r=1}^{n} \beta_r \mathbf{x}^{(r)},$$

where the β_r are constants. After p steps of the iteration, we have

$$y^{(p)} = A^{-1}y^{(p-1)} = \ldots = (A^{-1})^p y^{(0)}$$

$$= \sum_{r=1}^{n} \beta_r \alpha_r^{-p} \mathbf{x}^{(r)},$$

since $A\mathbf{x}^{(r)} = \alpha_r \mathbf{x}^{(r)}$, $A^2\mathbf{x}^{(r)} = \alpha_r^2 \mathbf{x}^{(r)}$ etc., the eigenvalues of A^{-1} are the reciprocals of those of A, and the eigenvectors of A^{-1} are the same as those of A.

Thus if α_1 is the eigenvalue of smallest modulus,

$$\mathbf{y}^{(p)} = \beta_1 \alpha_1^{-p} \left\{ \mathbf{x}^{(1)} + \sum_{r=2}^{n} \beta_r \left(\frac{\alpha_1}{\alpha_r} \right)^p \mathbf{x}^{(r)} \right\}.$$

The second term in the bracket on the right decreases as p increases, until for large p,

$$\mathbf{y}^{(p)} = \beta_1 \alpha_1^{-p} \mathbf{x}^{(1)} + \boldsymbol{\varepsilon}_1^{(p)}$$

where $\boldsymbol{\varepsilon}^{(p)}$ is a very small vector.

In practice, $\mathbf{y}^{(p)}$ is normalised with respect to its largest element after each step, in order to avoid the possibility of accumulator overflow in the computer, so that

$$\mathbf{y}^{(p)} = \alpha_1^{-1} \{ \mathbf{x}^{(1)} + \boldsymbol{\varepsilon}_1^{(p)} \},$$

where the largest element of $\mathbf{x}^{(1)}$ is unity, and $\boldsymbol{\varepsilon}_1^{(p)}$ is a very small vector. Provided the iteration is continued until $\boldsymbol{\varepsilon}_1^{(p)}$ is sufficiently small, the eigenvalue of smallest modulus is given by the inverse of the largest element of $\mathbf{y}^{(p)}$, and $\mathbf{y}^{(p)}$ is its associated eigenvector, which is determined to within a multiplicative constant.

Any eigenvalue α_m of the matrix A can be found by this process, by considering a matrix $B = (A - gI)$ where g is an estimate of α_m. Providing that g is a sufficiently close estimate of α_m for $(\alpha_m - g)$ to be the eigenvalue of B with smallest modulus, the inverse iteration,

$$B\mathbf{z}^{(p)} = \mathbf{z}^{(p-1)}, \qquad \mathbf{z}^{(0)} \text{ arbitrary},$$

with normalisation of $\mathbf{z}^{(p)}$ after each step will result in

$$\mathbf{z}^{(p)} = (\alpha_m - g)^{-1} \{ \mathbf{x}^{(m)} + \boldsymbol{\varepsilon}_m^{(p)} \}$$

where $\varepsilon_m^{(p)}$ is a very small vector and $\mathbf{x}^{(m)}$ has its largest element unity. Thus $\mathbf{z}^{(p)}$ is the eigenvector corresponding to the eigenvalue α_m, where $(\alpha_m - g)$ is the inverse of the largest element of $\mathbf{z}^{(p)}$.

The rate of convergence of the iteration mainly depends on, and decreases with, the ratio of the eigenvalue of smallest modulus to the eigenvalue of next smallest modulus. The computer program of Ref. 1 therefore uses an iteration with the matrix $E_0 - \lambda_0 I$, where λ_0 is a good estimate to λ, to get the iteration to converge quickly.

APPENDIX II

Comparison of F(u) at $\gamma = \pi/4$ Calculated by Different Methods

Calculations of the behaviour of the load near the apex have previously concentrated on finding the values of the exponents v_m rather than the factor f of the velocity potential. However, in the course of his calculation[4], Taylor obtains a series expansion for f, and Brown[8] has recently calculated values of f on the sector for the case $\gamma = \pi/4$. These results are used here to calculate the corresponding functions $F(u)$ for the case $\gamma = \pi/4$, so that a comparison can be made with $F(u)$ calculated by the method of Section 3.

The series expansion obtained by Taylor[9] for the function f on the sector surface is

$$f_s(t) = 0{\cdot}96612\left[\cos t - \frac{q}{16}N\cos 3t - q^2\left\{\frac{N}{8}\left(1+\frac{N}{32}\right)\cos 3t + \frac{N}{24}\left(1-\frac{N}{32}\right)\cos 5t\right\} - \right.$$

$$- q^3\frac{N}{16}\left\{\left(1+\frac{N}{12}+\frac{N^2}{768}\right)\cos 3t + \left(1-\frac{N}{36}-\frac{N^2}{576}\right)\cos 5t + \right.$$

$$\left.\left. + \left(\frac{1}{2}-\frac{N}{36}+\frac{N^3}{4608}\right)\cos 7t\right\}\ldots\right] \tag{II.1}$$

where $N = -8v(v+1)$ and q is a small parameter,

$$q = \exp(-\pi K'/K),$$

where K and K' are complete elliptic integrals of the first kind with moduli $k = \sin\gamma$ and $k' = \cos\gamma$. The variable t is given by

$$t = \frac{\pi}{2}\frac{v}{K}$$

where

$$dnv = \cos\theta = \frac{y_1}{r}. \tag{II.2}$$

From equation (8)

$$F(u) = \left\{\frac{u^{\frac{1}{2}}r}{v}\frac{\partial f}{\partial y_1} + u^{\frac{1}{2}}\cos\theta f\right\}_s$$

$$= \left\{\frac{u^{\frac{1}{2}}}{v}r\frac{\partial v}{\partial y_1}\frac{\partial f}{\partial v} + u^{\frac{1}{2}}\,dnv\,f\right\}_s. \tag{II.3}$$

The relation between the coordinates u and v can be derived using equation (4)

$$u = \frac{\cos\theta - \cos\gamma}{1 - \cos\theta\cos\gamma}$$

$$= \frac{dnv - k'}{1 - k'dnv} = \frac{h^2cn^2v}{(1-k'dnv)(dnv+k')} \tag{II.4}$$

Also, from equation (II.2)

$$r\frac{\partial v}{\partial y_1} = -\frac{snv}{cnv}.$$

Therefore, substituting into equation (II.3), we have

$$F(u) = \frac{1}{v}\frac{ksnv}{[(1 - k'dnv)(dnv + k')]^{\frac{1}{2}}}\left(-\frac{\partial f_s}{\partial v}\right) + dnv\left(\frac{dnv - k'}{1 - k'dnv}\right)^{\frac{1}{2}} f_s. \tag{II.5}$$

Values of $F(u)$ have been calculated for a range of values of u using the formulae (II.1) and (II.4) in equation (II.5) for the case when $\gamma = \pi/4$. For this case, $k = k' = 1/\sqrt{2}$, Taylor's value for v is 0·8146, and the parameter of the series expansion (II.1), q, has the very small value of 0·04321.

Brown has used the same coordinate, v, as Taylor in her calculation of values of f_s at a large number of equally spaced values of v over a sector with semi-apex angle $\pi/4$. Values of the function $F(u)$ have been calculated from equation (II.5) using a six-point Lagrangian differentiation formula to calculate the derivative $\partial f_s/\partial v$, and Brown's value for v, which is 0·81465.

The values of $F(u)$ from the three methods of Taylor, Brown and Section 3 are given in Table 2. It can be seen that the agreement between the three methods is extremely close, differences between the values of the functions being no larger than the differences in the value of v calculated by the different methods, which is only 0·00015.

APPENDIX III

Comparison of the Exponents ν_m Calculated by Different Methods

Since Ref. 2 was published, values of the exponents ν_m of the distance factor in the velocity potential eigenfunctions have been calculated by Taylor[4] and Sack[12]. Taylor's method of calculation involves separation of the variables to obtain two Lamé equations which have two separation constants, one of which is $\nu_m(1 + \nu_m)$. He obtains a series solution for each Lamé equation in a small parameter, combines these to eliminate one separation constant and thus obtains an equation which can be solved for ν_m.

Sack considers the same Lamé equations as Taylor, but treats each equation as having an eigenvalue and a common separation constant, Λ, which is $\nu_m(1 + \nu_m)$. He describes a method for finding the eigenvalue of each Lamé equation for a given value of Λ. This involves expanding the eigenfunction as a Fourier series. The vector whose elements are the coefficients of this Fourier series is then the eigenvector of an infinite matrix. The corresponding eigenvalue can be found by truncating the matrix to finite size and then using a standard numerical method. In order to solve both Lamé equations simultaneously, Sack considers the linear equation connecting the two eigenvalues of the two Lamé equations and the separation constant Λ as a function of Λ, solves it for Λ using Newton's method and hence finds the value of ν_m.

From the point of view of further developments, it is noteworthy that neither Taylor nor Sack restricts his eigensolutions to even functions of y_2, corresponding to flows with lateral symmetry. However, the method of Ref. 2 and the present Report considers the case appropriate to flow over the apex of a wing and so restricts the velocity potentials considered to those which are even functions of y_2.

In this Appendix, we take the opportunity to compare the results of different calculations of the first two eigenvalues ν_0 and ν_1 corresponding to symmetrical velocity potentials.

Figs. 9 to 12 compare the values of ν_0 and ν_1, over a range of values of semi-apex angle γ, given by the calculations of Brown and Stewartson[3], Taylor[4], Sack[12] and Rossiter[2]. Extremely good agreement is obtained for ν_0, *see* Figs. 9 and 10, although for small semi-apex angles, ν_0 is not given by Rossiter's method and is over-estimated by Taylor's. Values of ν_1 for γ greater than $\pi/2$ calculated by Sack and Rossiter are also in good agreement, see Fig. 11, although Rossiter's method does not give values for γ near π. Taylor's results agree for semi-apex angles between about 120 and 145 degrees but lose accuracy outside this range. For γ less than $\pi/2$, *see* Fig. 12, only Sack and Taylor have calculated values of ν_1 over the whole range of semi-apex angles. These are in good agreement for γ greater than $\pi/4$, and exponents calculated by the other methods at $\gamma = 45$ and 81 degrees also agree well. However, Taylor's method is not accurate for semi-apex angles below $\pi/6$. Taylor attributes this loss in accuracy to the fact that the parameters of the series solutions for the Lamé equations are no longer sufficiently small for γ not close to $\pi/4$ or $3\pi/4$, this effect being more serious for the higher eigenvalues, i.e. $\nu_m > 1$. Sack also gives reasons for believing his calculation method to be more accurate than Taylor's.

TABLE 1

Coefficients of Cubic Polynomial Approximation for F(u)

$$F(u) = a_0 + a_1 u + a_2 u^2 + a_3 u^3$$

Semi-apex angle γ^0	Exponent ν	a_0	a_1	a_2	a_3	Section describing method of calculation
90	0·5	1·0	0	0	0	4·3
81	0·5526	0·94957	0·04525	0·00777	−0·00259	
72	0·6109	0·89894	0·09880	0·00557	−0·00331	
63	0·6749	0·84982	0·15728	−0·00624	−0·00086	
54	0·7441	0·80375	0·21709	−0·02391	0·00307	3
45	0·8145	0·76493	0·26996	−0·04325	0·00836	
36	0·8808	0·73558	0·31087	−0·05890	0·01245	
27	0·9356	0·71740	0·33665	−0·06948	0·01543	
		0·71732	0·33708	−0·07005	0·01565	
18	0·9731	0·70934	0·34843	−0·07457	0·01680	4·1
9	0·9936	0·70731	0·35133	−0·07576	0·01712	
0	1·0	0·70711	0·35162	−0·07589	0·01716	4·2

TABLE 2

F(u) at $\gamma = \pi/4$ calculated by different methods

u	$F(u)$ by method of		
	Taylor	Brown	Section 3
0	0·7650	0·7650	0·7649
0·0122	0·7681	0·7681	0·7682
0·0494	0·7781	0·7780	0·7782
0·1134	0·7949	0·7949	0·7950
0·2064	0·8188	0·8188	0·8189
0·3300	0·8495	0·8495	0·8496
0·4827	0·8860	0·8860	0·8861
0·6549	0·9255	0·9255	0·9255
0·8235	0·9626	0·9626	0·9626
0·9515	0·9899	0·9899	0·9899
1·0	1·0	1·0	1·0

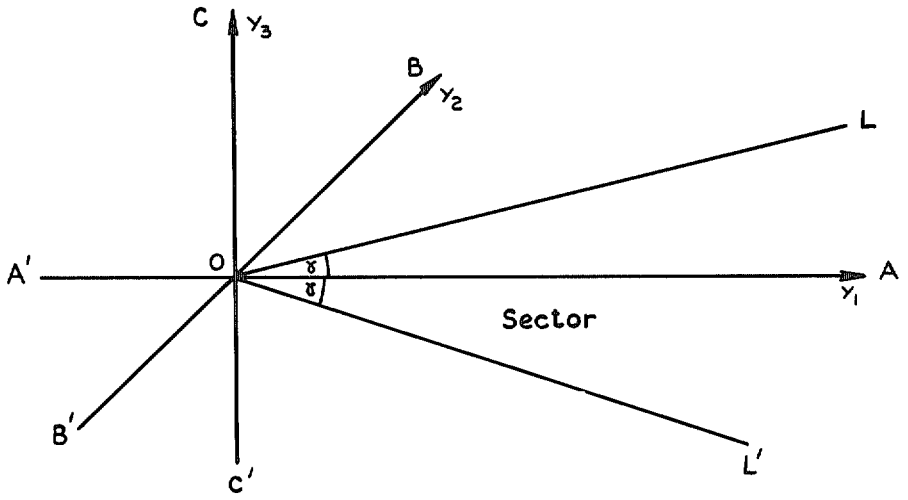

FIG. 1. (y_1, y_2, y_3) coordinate system.

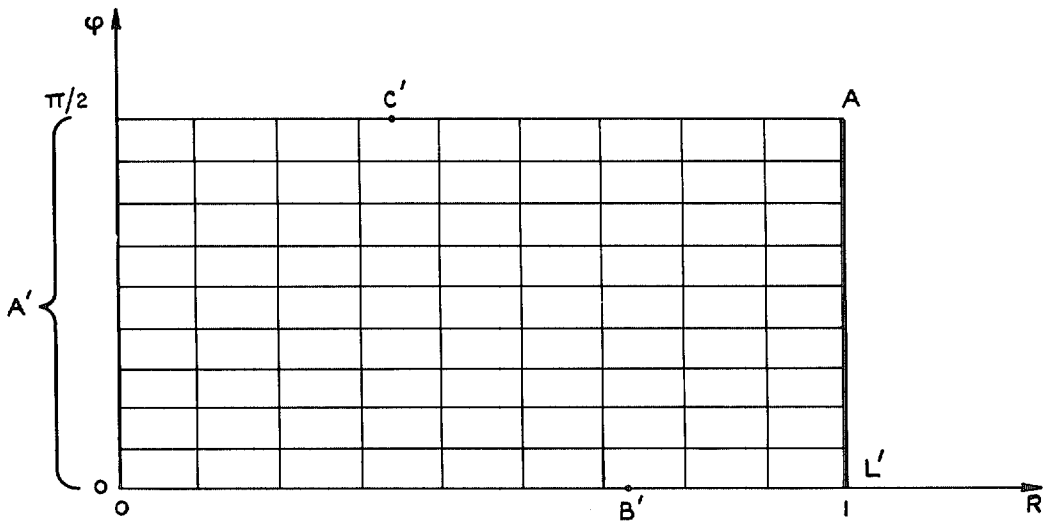

FIG. 2. The grid in the R, φ plane for $l = 9$.

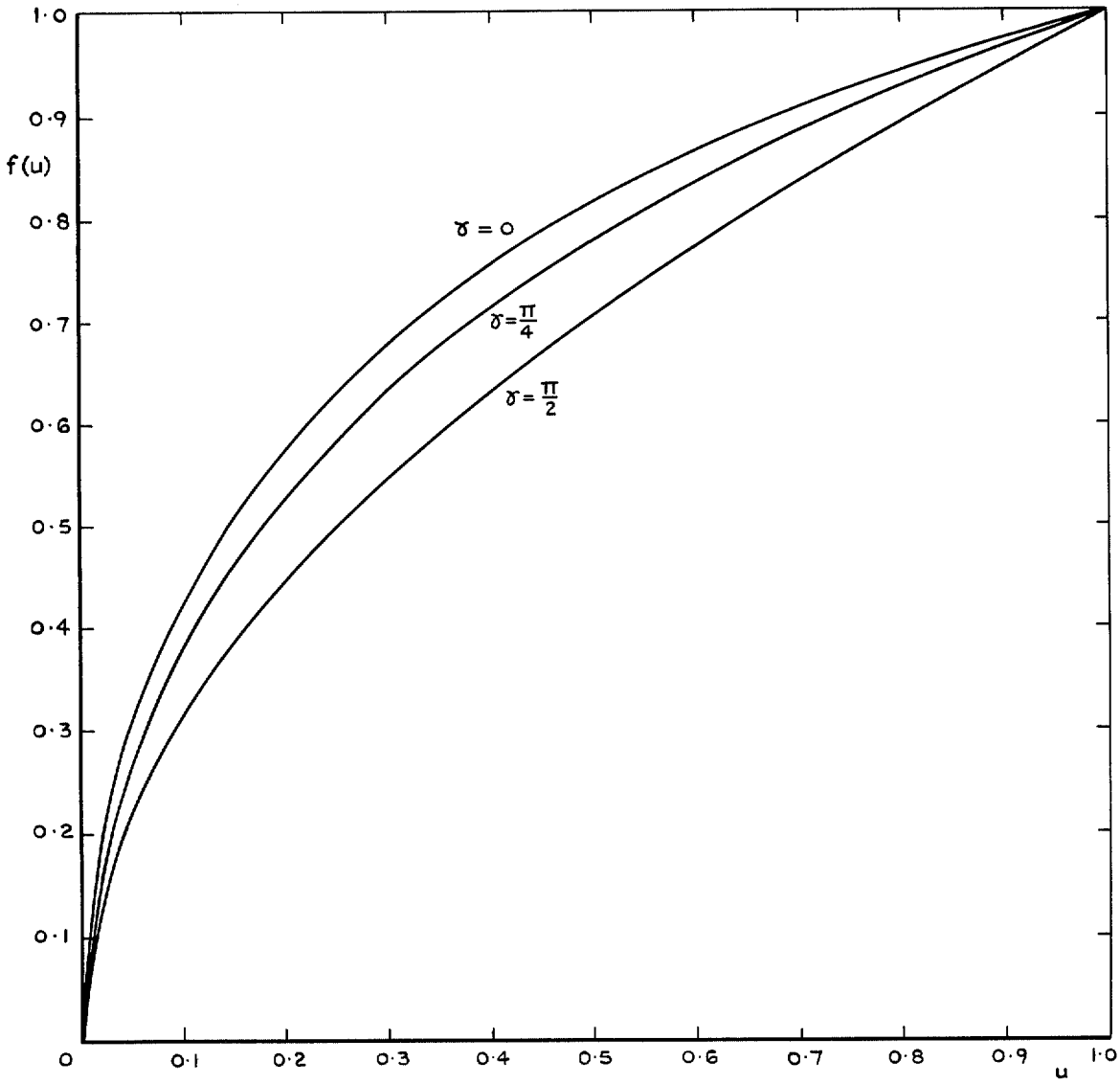

FIG. 3. The factor f in the velocity potential near the apex for various semi-apex angles.

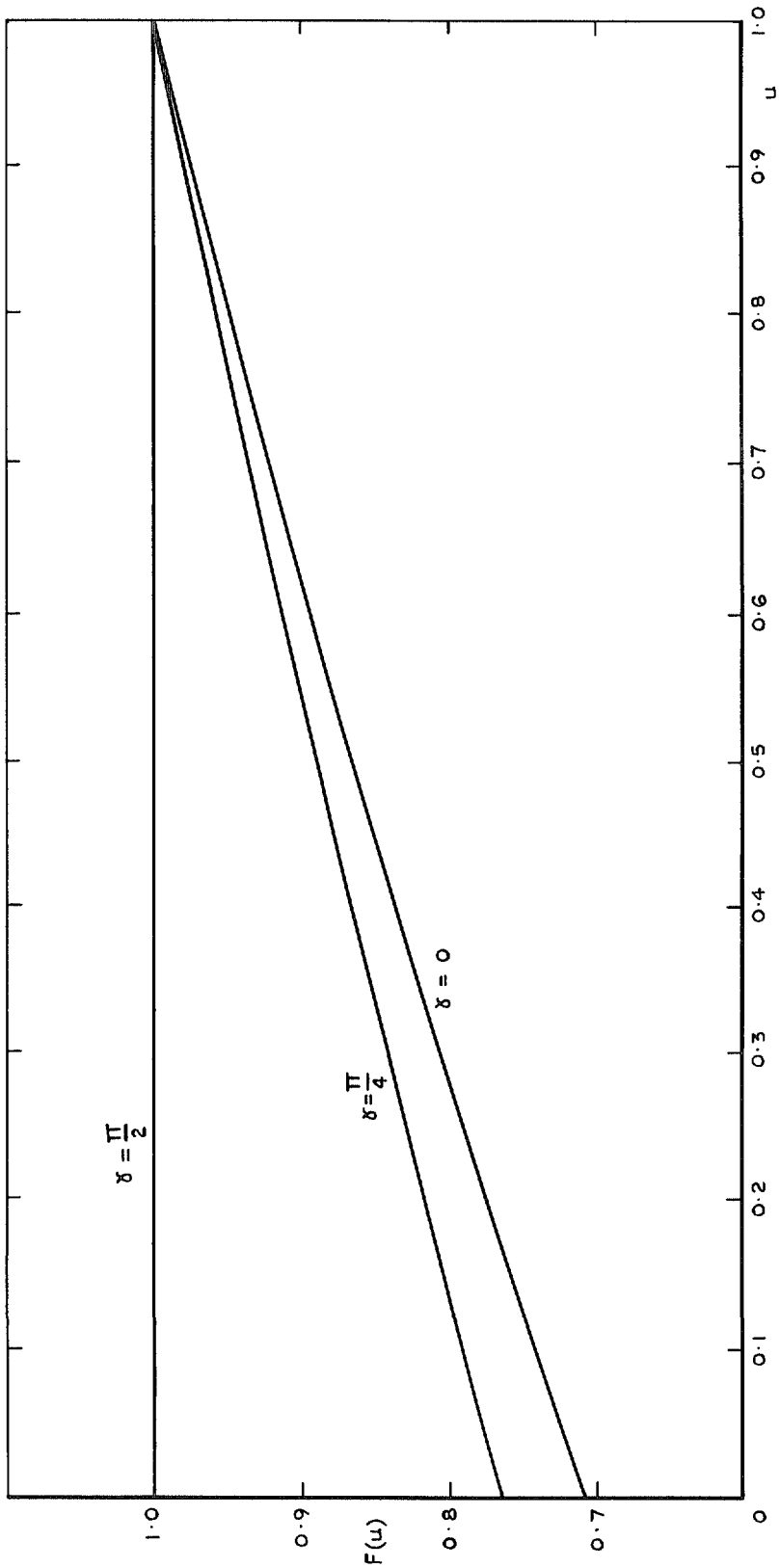

FIG. 4. The factor $F(u)$ of the load near the apex for various semi-apex angles.

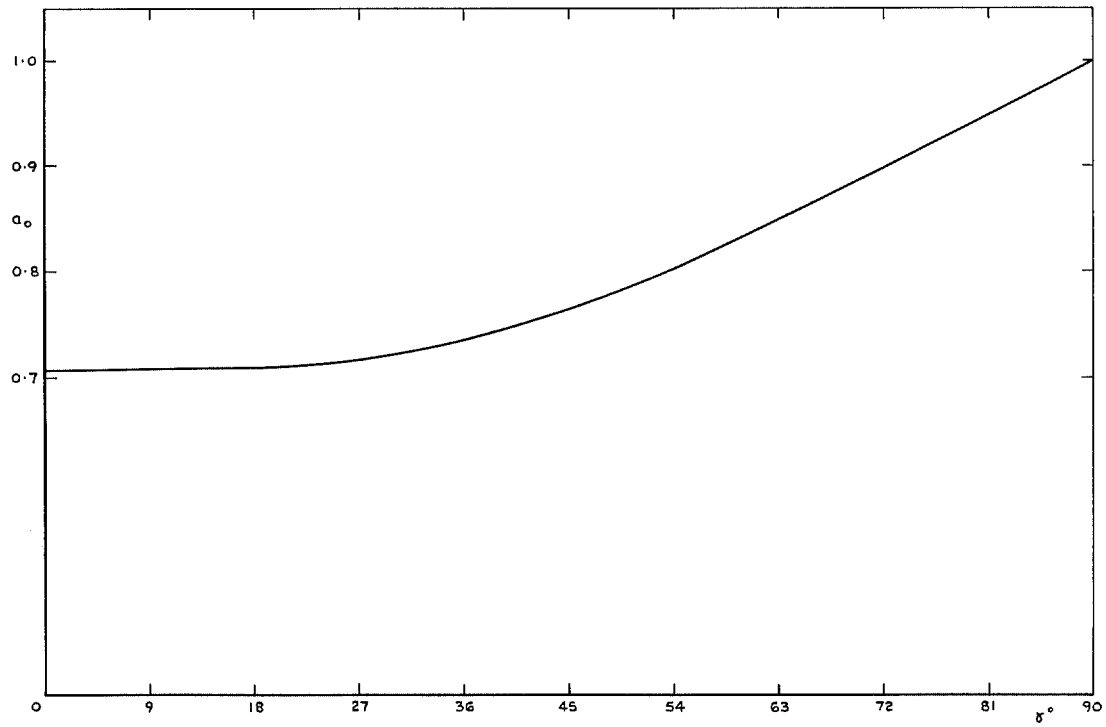

FIG. 5. Variation of a_0 with semi-apex angle.

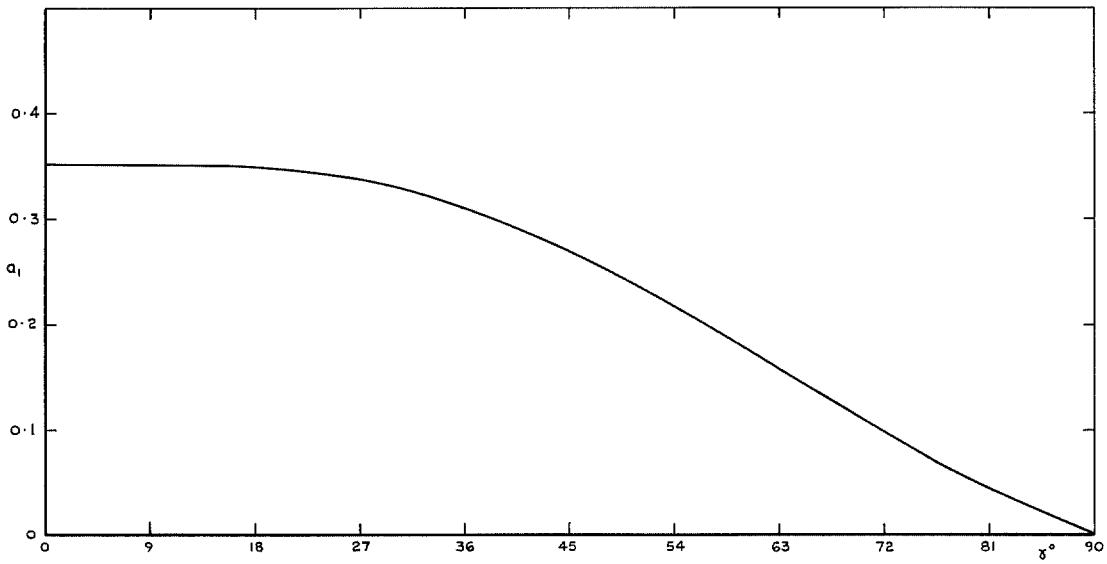

FIG. 6. Variation of a_1 with semi-apex angle.

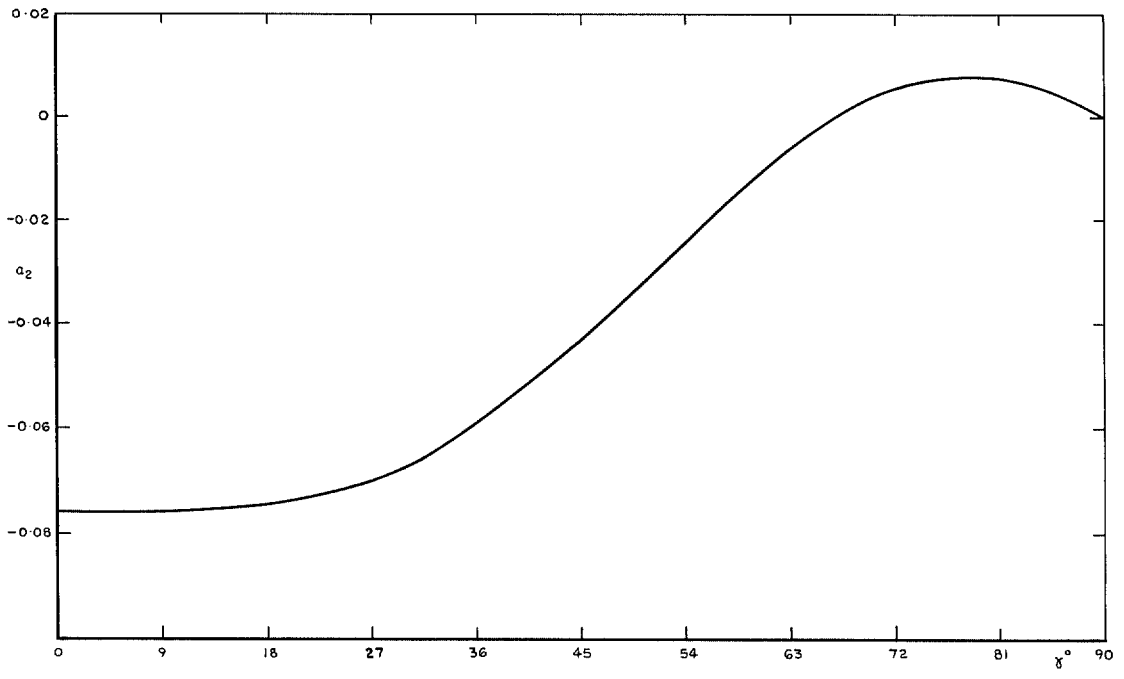

FIG. 7. Variation of a_2 with semi-apex angle.

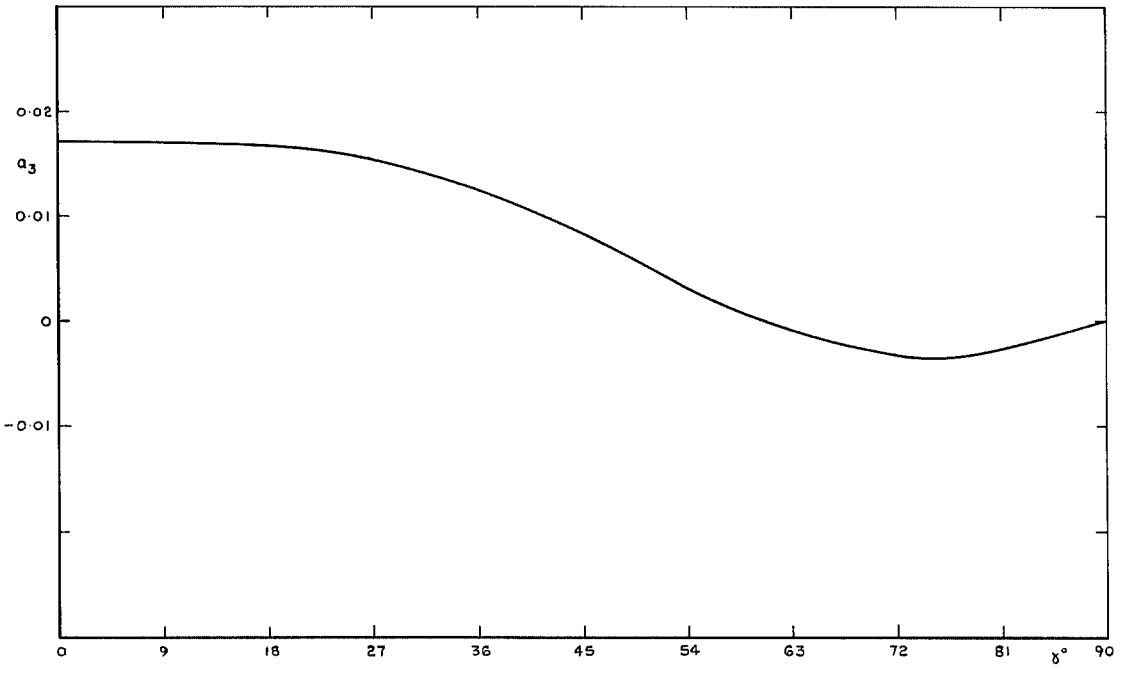

FIG. 8. Variation of a_3 with semi-apex angle.

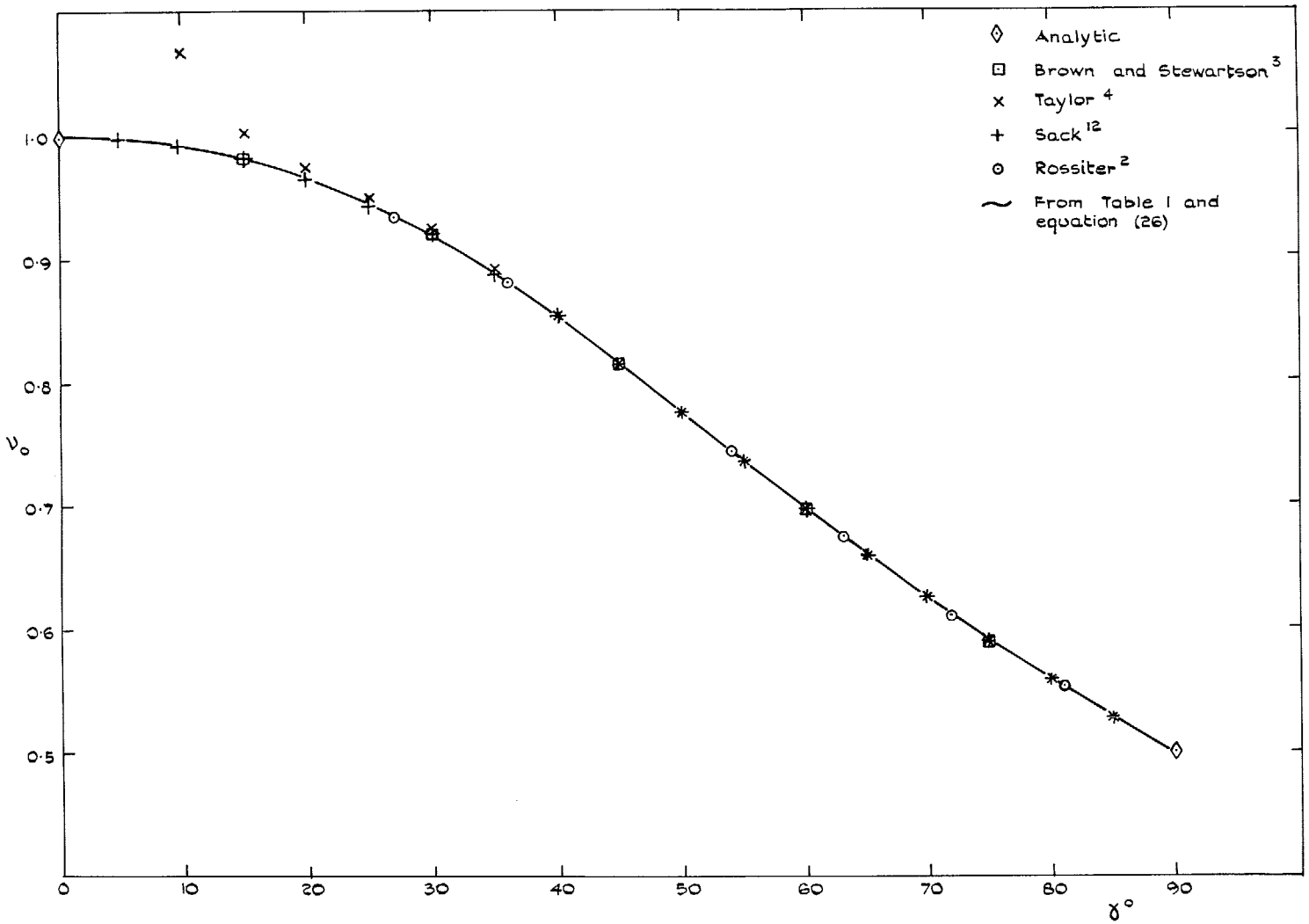

FIG. 9. Comparison of first eigenvalue for $0 \leqslant \gamma \leqslant \pi/2$, calculated by different methods.

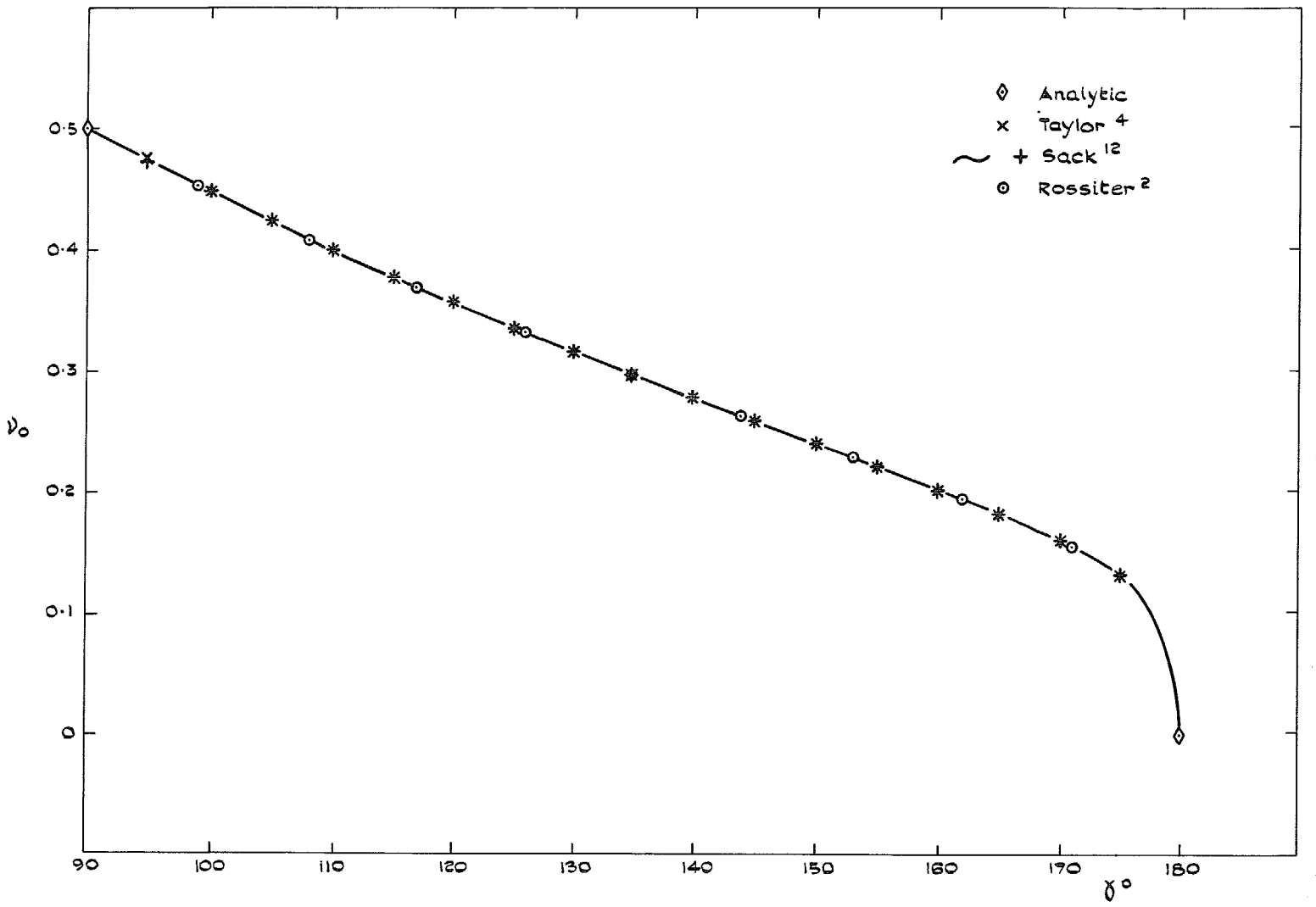

FIG. 10. Comparison of first eigenvalue for $\pi/2 \leqslant \gamma \leqslant \pi$, calculated by dfferent methods.

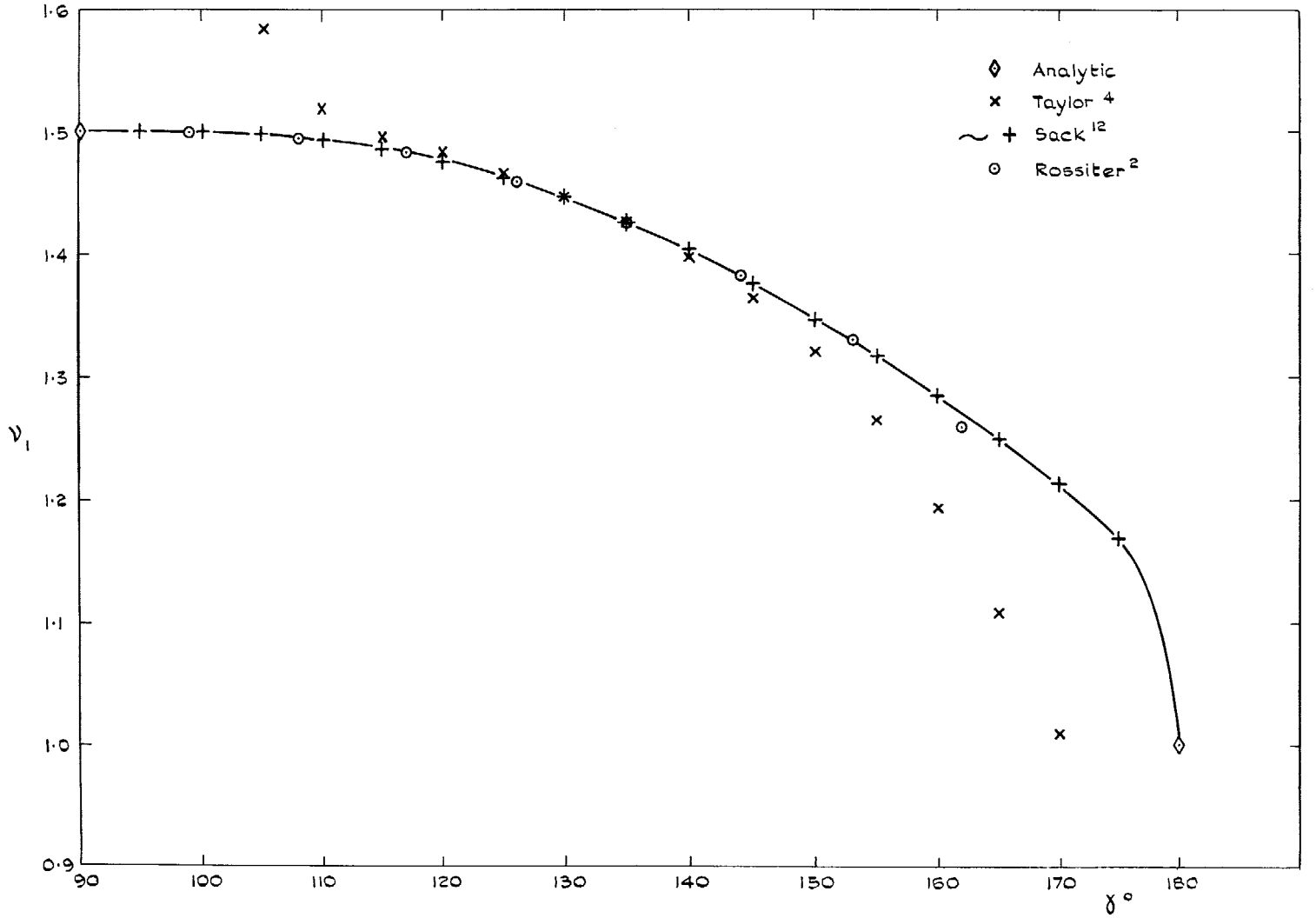

FIG. 11. Comparison of second (trailing edge) eigenvalue for $\pi/2 \leqslant \gamma \leqslant \pi$, calculated by different methods.

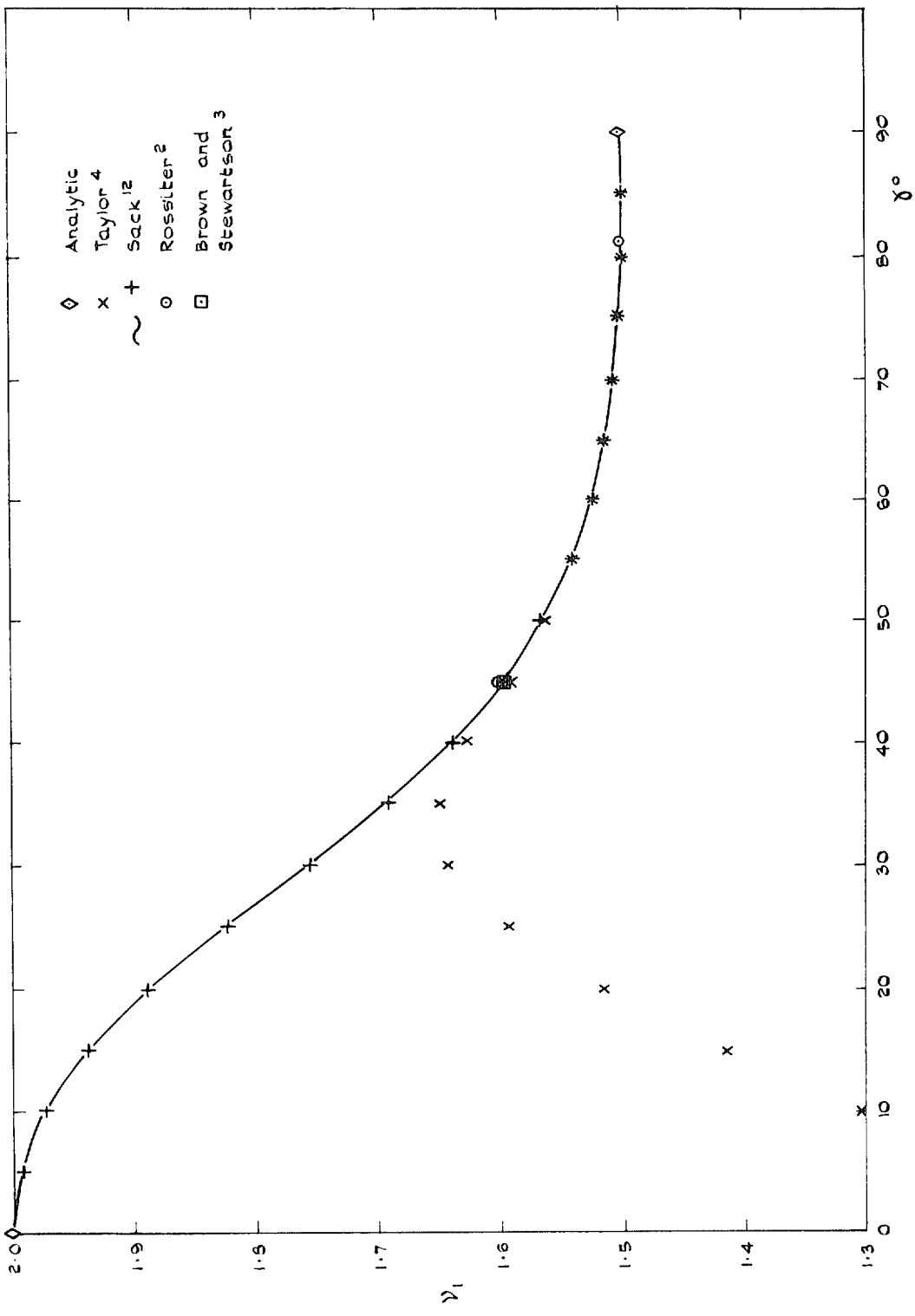

FIG. 12. Comparison of second eigenvalue for $0 \leqslant \gamma \leqslant \pi/2$, calculated by different methods.

Printed in England for Her Majesty's Stationery Office by J. W. Arrowsmith Ltd., Bristol
Dd. 503426 K.5 1/73

HER MAJESTY'S STATIONERY OFFICE

Government Bookshops

49 High Holborn, London WC1V 6HB
13a Castle Street, Edinburgh EH2 3AR
109 St Mary Street, Cardiff CF1 1JW
Brazennose Street, Manchester M60 8AS
50 Fairfax Street, Bristol BS1 3DE
258 Broad Street, Birmingham B1 2HE
80 Chichester Street, Belfast BT1 4JY

Government publications are also available through booksellers

SBN 11 470516 X